Published OnlineFirst November 10, 2009; DOI: 10.1158/0008-5472.CAN-09-1968

Differential Enhancement of Breast Cancer Cell Motility and Metastasis by Helical and Kinase Domain Mutations of Class IA Phosphoinositide 3-Kinase

Huan Pang,[1] Rory Flinn,[1] Antonia Patsialou,[2] Jeffrey Wyckoff,[2] Evanthia T. Roussos,[2] Haiyan Wu,[1] Maria Pozzuto,[3] Sumanta Goswami,[4] John S. Condeelis,[2] Anne R. Bresnick,[3] Jeffrey E. Segall,[2] and Jonathan M. Backer[1]

Departments of [1]Molecular Pharmacology, [2]Anatomy and Structural Biology, and [3]Biochemistry, Albert Einstein College of Medicine, Bronx, New York and [4]Department of Biology, Yeshiva University, New York, New York

Abstract

Class IA (p85/p110) phosphoinositide 3-kinases play a major role in regulating cell growth, survival, and motility. Activating mutations in the p110α isoform of the class IA catalytic subunit (PIK3CA) are commonly found in human cancers. These mutations lead to increased proliferation and transformation in cultured cells, but their effects on cell motility and tumor metastasis have not been evaluated. We used lentiviral-mediated gene transfer and knockdown to produce stable MDA-MB-231 cells in which the endogenous human p110α is replaced with either wild-type bovine p110α or the two most common activating p110α mutants, the helical domain mutant E545K and the kinase domain mutant H1047R. The phosphoinositide 3-kinase/Akt pathway was hyperactivated in cells expressing physiologic levels of helical or kinase domain mutants. Cells expressing either mutant showed increased motility *in vitro*, but only cells expressing the helical domain mutant showed increased directionality in a chemotaxis assay. In severe combined immunodeficient mice, xenograft tumors expressing either mutant showed increased rates of tumor growth compared with tumors expressing wild-type p110α. However, tumors expressing the p110α helical domain mutant showed a marked increase in both tumor cell intravasation into the blood and tumor cell extravasation into the lung after tail vein injection compared with tumors expressing wild-type p110α or the kinase domain mutant. Our observations suggest that, when compared with kinase domain mutations in a genetically identical background, expression of helical domain mutants of p110α produce a more severe metastatic phenotype. [Cancer Res 2009;69(23):8868–76]

Introduction

Phosphoinositide 3-kinases (PI3K) signal to multiple downstream pathway by the specific phosphorylation of the D3 position of the inositol headgroup. The class IA isoforms contain distinct regulatory (p85α, p85β, p55α, and p50γ) and catalytic (p110α, p110β, and p110δ) subunits. The p85α and p110α isoforms are mutated in human cancers, and the p110α mutants are oncogenic *in vitro* and *in vivo* (1).

The bulk of p110α mutations occurs at two hotspots: an acidic cluster in the helical domain (E542, E545, and E546) and a residue in the kinase domain (H1047). Zhao and Vogt have shown that the E545K and H1047R mutants synergistically induce transformation in chick fibroblasts (2), suggesting that these mutations activate PI3K in mechanistically distinct manners. The helical domain mutations disrupt an inhibitory interface with the nSH2 domain of the p85, mimicking the effect of phosphotyrosine protein binding to the nSH2 domain (3). Consistent with this model, helical domain mutants are not activated by tyrosyl phosphopeptides but are activated by oncogenic Ras, which binds to the Ras-binding domain of p110α (2, 4). In contrast, the p110α H1047R mutant is still inhibited by p85,[5] and p85/p110 dimers containing the H1047R mutant are activated by phosphopeptides (5). However, p85/p110α H1047R mutants are not activated by oncogenic Ras, suggesting that the H1047R mutation mimics the effects of Ras binding to the Ras-binding domain of p110α (2, 4).

These different mechanisms of activation could lead to different localization of PI3K activity in the cell. Both mutants bind to p85 and would be recruited to sites of receptor or docking protein tyrosine phosphorylation in growth factor–stimulated cells. However, recruitment of a helical domain mutant to a tyrosine-phosphorylated receptor would not lead to a gradient of PI3K activity, because these mutants are not additionally activated by SH2 domain occupancy (3). In contrast, kinase domain mutants are activated by SH2 domain occupancy and would be more active at the site of recruitment than in the cytosol (5). Additional differences in the activity of membrane-targeted versus cytosolic PI3K would be caused by binding to GTP-Ras; helical domain mutants would show increased activity on targeting to a Ras-rich membrane domain, whereas kinase domain mutants would not (2, 4). Given recent studies showing activation of Ras isoforms in distinct membrane domains (6), this could also lead to different gradients of cytosolic versus membrane-targeted activity for the two types of mutant.

Although overexpression of either helical versus kinase domain mutants of p110α causes increased cell growth and transformation (7–10), studies using different methods to introduce mutant p110α have yielded discordant results as to whether their phenotypes differ *in vivo* (11, 12). However, Saal and colleagues defined a gene expression signature indicative of a loss of PTEN-mediated inhibition of PI3K signaling (13); of tumors showing both PTEN

Note: Supplementary data for this article are available at Cancer Research Online (http://cancerres.aacrjournals.org/).

Requests for reprints: Jonathan M. Backer, Department of Molecular Pharmacology, Albert Einstein College of Medicine, 1300 Morris Park Avenue, Bronx, NY 10461. Phone: 718-430-2153; Fax: 718-430-3749; E-mail: backer@aecom.yu.edu.

doi:10.1158/0008-5472.CAN-09-1968

[5] J.M. Backer, unpublished data.

Published OnlineFirst November 10, 2009; DOI: 10.1158/0008-5472.CAN-09-1968

loss signature and mutation of p110α, 67% of the tumors contained kinase domain mutants, and only 19% contained helical domain or C2 domain mutants. These data strongly suggest that helical and kinase domain mutants have distinct physiologic phenotypes in human cancers.

This study specifically examines the contribution of helical domain versus kinase mutations in p110α to the metastatic properties of human breast cancer cells. To address this question, we used the human cell line MDA-MB-231, which is capable of producing tumors in severe combined immunodeficient (SCID) mice but is normal for both PI3K and PTEN. Using a lentiviral strategy, we stably replaced endogenous human p110α with physiologic levels of wild-type or mutant bovine p110α. Both helical domain and kinase domain mutants cause similar increases in tumor growth *in vivo* compared with cells expressing wild-type p110α. However, cells expressing helical domain mutants are more chemotactic *in vitro* and show markedly increased rates of intravasation and extravasation *in vivo*. These data suggest that helical domain mutants of p110α confer an increased metastatic potential, which could have important implications for the prognosis of patients whose tumors contain p110α mutations.

Materials and Methods

Antibodies. Affinity-purified rabbit antibodies against p110α and p85α have been described previously (14). Mouse anti-myc antibodies were produced in-house. Anti-pAkt and anti-Akt antibodies were purchased from Cell Signaling Technology.

Lentiviral constructs and lentivirus generation. Bovine p110α bearing a COOH-terminal myc tag was subcloned into a modified lentiviral vector with a blasticidin selection marker (15). The oncogenic mutations E545K and H1047R and kinase-disabling mutation R916P were introduced into p110α using QuikChange site-directed mutagenesis kit (Stratagene) and confirmed by sequencing. Human p110α short hairpin RNAs in pLKO.1-puro vector were purchased from Sigma. To package the lentivirus, HEK293T cells were transfected with lentiviral vectors encoding no insert, wild-type, or mutant bovine p110α, or short hairpin RNA against human p110α, along with the packaging vectors pVSVG and pCMVdR. Recombinant lentivirus was collected from the tissue culture supernatant 48 h after transfection.

Cell culture and stable cell lines. The human breast cancer cell line MDA-MB-231 was obtained from the American Type Culture Collection and maintained in monolayer cultures in DMEM supplemented with 10% fetal bovine serum. Cells were infected at various multiplicities of infection with lentivirus expressing wild-type or mutant COOH-terminally myc-tagged bovine p110α and selected with blasticidin. Resistant populations were blotted with anti-myc antibody to identify lines in which myc-tagged bovine p110α expression was at a physiologic level. The stable lines were then subjected to a second infection with lentivirus expressing short hairpin RNA against human p110α and then selected with puromycin. Stable knockdown of human p110α was determined by real-time PCR and by Western blot analysis of parallel cultures of cells not expressing bovine p110α. This procedure resulted in four cell lines that had been subjected to sequential stable lentiviral bovine p110α transfection and human p110α knockdown. As a control, cell lines in which stable knockdown was followed by expression of helical or kinase domain mutants of p110α were also evaluated *in vitro* for p110 expression, Akt phosphorylation, protrusion, motility, and wound healing and showed similar results to cell lines obtained using the replacement strategy (Supplementary Figs. S1 and S2).

Immunoprecipitation and Western blots. Stable cells were rinsed in cold PBS and lysed in a buffer containing 120 mmol/L NaCl, 20 mmol/L Tris (pH 7.5), 1 mmol/L $MgCl_2$, 1 mmol/L $CaCl_2$, 10% glycerol, 1% NP-40, 1 mmol/L DTT, and protease inhibitor cocktail (Roche). Proteins were immunoprecipitated with anti-myc, anti-p85, anti-p110α, anti-p110β (all produced in-house), or anti-p110δ (Epitomics) antibodies. Blots were probed with anti-p85, anti-p110α (produced in-house), or anti-p110δ (Epitomics) antibodies. For Akt immunoblots, stable MDA-MB-231 lines were starved for 4 h in starvation medium (DMEM/0.5% fetal bovine serum/0.8% bovine serum albumin), stimulated without or with 5 nmol/L epidermal growth factor (EGF) for 3 min, and immediately lysed in hot sample buffer. Proteins were separated by 10% SDS-PAGE, and anti-Akt and anti-pAkt (Cell Signaling Technology) blots were visualized using enhanced chemiluminescence (Amersham).

Anti–phosphatidylinositol-3,4,5-trisphosphate staining. Cells were fixed and stained as described previously using anti–phosphatidylinositol-3,4,5-trisphosphate (PIP_3) antibodies (Echelon; ref. 16).

Protrusion assays. Stable MDA-MB-231 cells were seeded in 35 mm dish coated with Matrigel. After 12 h of adhesion, cells were incubated in starvation medium for 4 h and stimulated with 2.5 nmol/L EGF (Invitrogen). Phase-contrast time-lapse images of the cells were collected every 20 s and digitized using a Scion frame-grabber. Cell surface area changes were analyzed using NIH ImageJ software.

Boyden chamber assay. Transwell chambers (6.5 mm diameter, 8 μm pore size; Costar) were coated with collagen I (BD Bioscience) overnight and then rinsed with medium plus 0.8% bovine serum albumin before use. MDA-MB-231 cells expressing wild-type or mutant p110α (5×10^4 per well) were applied to the top chamber in starvation medium. EGF (0 or 2.5 nmol/L) was added to the bottom chamber as a chemoattractant. After 4 h migration at 37°C, cells in the bottom surface were fixed, stained with 4′,6-diamidino-2-phenylindole, and counted.

Wound-healing assay. Cells were grown to confluency on culture plates and a wound was made in the monolayer with a sterile P200 pipette tip (~0.5 mm in width). After wounding, the cells were washed to remove debris and new medium was added. Phase-contrast images of the wounded area were taken at 0, 4, and 20 h after wounding. Wound widths were measured at a minimum of 10 different points for each wound, and the average rate of wound closure during the first 4 h of wound healing was calculated.

Dunn chamber chemotaxis assay. Cells (2×10^5 per dish) were seeded onto the Matrigel-coated coverslips and allowed to attach overnight. The next day, cells were starved for 4 h in starvation medium, and the coverslips with attached cells were inverted and mounted onto a Dunn chemotaxis chamber (Hawksley Technology) as described (17). The inner well of the chamber was filled with starvation medium only, whereas the outer well was filled with starvation medium containing 5 or 0.5 nmol/L EGF as a chemoattractant as indicated. Time-lapse images of moving cells were recorded every 2 min over a 3 h period. Cells movements were tracked manually, and analyses of migration and chemotaxis was done using Mathematica notebooks written and provided by Profs. G.A. Dunn and G.E. Jones (King's College London; ref. 18).

Animal models. Xenograft tumors were produced by injection of 1×10^6 MDA-MB-231 cells expressing wild-type or mutant bovine p110α into the mammary glands of 5- to 7-week-old female SCID mice (19). Tumors size was measured weekly. The mice were sacrificed when tumors reached 1.2 to 1.3 cm in diameter.

Tumor cell blood burden. The blood burden of tumor cells were measured as described (20). SCID mice bearing xenograft tumors were anesthetized with isoflurane and blood was drawn from the right ventricle of the heart using a heparin-coated 25-gauge needle and a 1 mL syringe. Blood was placed in a tissue culture dish containing DMEM with 10% fetal bovine serum and incubated overnight. The dishes were rinsed with PBS twice on the following day and the DMEM was replaced every 3 days thereafter. Puromycin was added to the medium on the 5th day and colonies were counted on the 14th day. Each colony was scored as representing one tumor cell from the blood, and the numbers were normalized to the blood volume taken from the heart.

Lung metastases. MDA-MB-231 cells (1×10^6) stably expressing wild-type or mutant bovine p110α were injected i.v. into the tail vein of SCID mice. After 4 weeks (5 animals per groups) or 7 weeks (at least 3 animals per group), the mice were sacrificed. Lungs were collected, fixed in 10% neutral buffered formalin, and embedded in paraffin followed by serial sectioning. Five sections (100 μm apart) from each lung were stained with H&E and photographed. The tumor nodules were quantified by using ImageJ software.

Published OnlineFirst November 10, 2009; DOI: 10.1158/0008-5472.CAN-09-1968

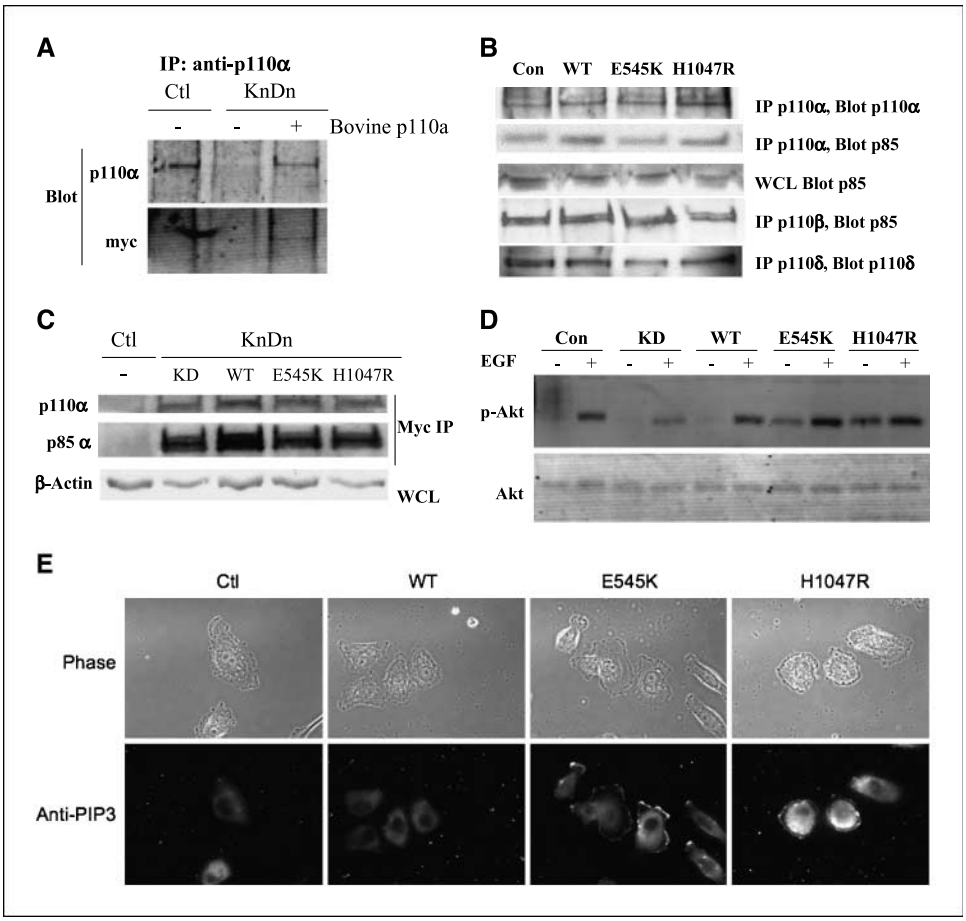

Figure 1. p110α expression, Akt phosphorylation, and PIP_3 production in cell lines expressing mutant bovine p110α in place of wild-type. *A,* anti-p110α immunoprecipitates were prepared from control MDA-MB-231 cells, cells infected with a lentiviral short hairpin RNA construct targeting human p110α, or cells in which human p110α was rescued with wild-type bovine p110α. The immunoprecipitates were immunoblotted with anti-p110α (*top*) or anti-myc (*bottom*) antibody. *B,* control cells or stable MDA-MB-231 cells in which human p110α was replaced with wild-type or mutant bovine p110α (helical domain, E545K; kinase domain, H1047R; kinase dead, KD) were immunoprecipitated with anti-p110α/β/δ antibodies. Immunoprecipitates or whole-cell lysates were blotted for p110α/δ or p85. *C,* control cells or stable MDA-MB-231 cells in which human p110α was replaced with wild-type or mutant bovine p110α were immunoprecipitated with anti-myc antibody and blotted with anti-p110α (*top*) or anti-p85α (*middle*) antibodies. Whole-cell lysates from these cell lines were blotted with anti–β-actin (*bottom*) as a loading control. *D,* control MDA-MB-231 cells or cells in which human p110α was replaced with bovine wild-type or mutant p110α were starved in starvation medium for 4 h and stimulated without or with 5 nmol/L EGF for 3 min. Equal amount of cell lysate was separated by 10% SDS-PAGE and blotted for pS473-Akt or total Akt. *E,* control MDA-MB-231 cells or cells in which human p110α was replaced with bovine wild-type or mutant p110α were serum-starved overnight, fixed, and stained with anti-PIP_3 antibody as described. Phase-contrast and immunofluorescence images for each cell line are shown.

Statistics. Quantitative data are expressed as mean ± SE. Statistical analysis was done using ANOVA, unpaired Student's *t* test, or Mann-Whitney *U* test. $P < 0.05$ was considered statistically significant.

Results

Replacement of endogenous p110α with wild-type or mutant bovine p110α in MDA-MB-231 cells. To test the effect of distinct oncogenic p110α mutations on motility and metastasis, we established stable MDA-MB-231 cell lines in which endogenous human p110α was replaced with wild-type or mutant bovine p110α. We used an approach similar to a knockdown/rescue strategy, except that we first expressed wild-type or mutant bovine p110α, and then knocked down the endogenous human p110α. This avoids possible adaptive responses to survival in the absence of p110α during the knockdown phase. The MDA-MB-231 line was chosen because it is capable of forming tumors in SCID mice but has normal alleles for both p110α and PTEN.[6] The mutants tested are the two most commonly mutated sites in p110α, E545K in the helical domain and H1047R in the kinase domain. The replacement strategy was accomplished using lentiviral-mediated gene transfer as described in Materials and Methods. Cells infected with empty viruses were used as controls.

Infection of control MDA-MB-231 with lentivirus expressing p110α short hairpin RNA caused >90% knockdown at the protein level as shown by immunoprecipitation with anti-p110α antibody and blots with anti-p110α antibody (Fig. 1*A*); knockdown was 70% efficient at the mRNA level as detected by real-time PCR (data not shown). In a traditional knockdown/rescue strategy, exogenous bovine p110α would be expressed at a level comparable with that of endogenous human p110α in control cells as detected by blotting with anti-p110α antibody (Fig. 1*A*). Similarly, in the p110α replacement cell lines used in this study, knockdown of human p110α was 80% efficient by real-time PCR (data not shown), and total levels of bovine p110α were similar to that of human p110α in control cells

[6] http://www.sanger.ac.uk/perl/genetics/CGP/cosmic?action=sample&id=905960

Published OnlineFirst November 10, 2009; DOI: 10.1158/0008-5472.CAN-09-1968

(Fig. 1*B*). Levels of total p85, p110β, and p110δ were also similar to that seen in control cells (Fig. 1*B*). Anti-myc immunoprecipitates from cell lines in which human p110α was replaced with wild-type or mutant bovine p110α also showed similar levels of bovine myc-p110α expression and myc-p110α-associated p85 (Fig. 1*C*). Thus, the stable cell lines expressed bovine p110α at physiologic levels.

Consistent with the p110α expression data, EGF-stimulated phosphorylation of Akt was significantly decreased in cells in which p110α was replaced with a kinase-dead mutant, whereas cells expressing wild-type bovine p110α showed a level of Akt phosphorylation similar to that seen in control cells (Fig. 1*D*). In contrast, MDA-MB-231 cells expressing either helical domain or kinase domain p110α mutants showed elevated basal levels of Akt phosphorylation as well as enhanced EGF-stimulated Akt phosphorylation. We also measured production of PIP_3 by immunofluorescence analysis of fixed cells using a previously characterized antibody specific for PIP_3 (16). In quiescent cells, PIP_3 was clearly increased in cells expressing helical and kinase domain mutants of p110α (Fig. 1*E*). These results show that PI3K signaling is increased in cells expressing the p110α E545K or H1047R mutants at physiologic levels.

p110α oncogenic mutants cause enhanced EGF-stimulated protrusion and cell motility. Actin-mediated protrusion at the leading edge of moving cells is an early step in carcinoma cell motility (21). The EGF-stimulated protrusion of MD-MBA-231 lines was measured by time-lapse video microscopy. Cells in which human p110α was replaced with wild-type bovine p110α showed a rate and extent of protrusion that was similar to control MDA-MB-231 cells. Cells expressing a kinase-dead p110α mutant showed minimal protrusion after EGF stimulation. This result is similar to our previous finding that the p110α isoform is required for EGF-stimulated protrusion in carcinoma cells (14). Cells expressing either helical domain (E545K) or kinase domain (H1047R) mutants exhibited significantly greater protrusion in response to EGF compared with control cells (Fig. 2*A*). These results indicate that oncogenic p110α mutants promote cell protrusion in carcinoma cells.

To test the effects of mutant p110α on cell motility, we evaluated MDA-MB-231 cells expressing wild-type p110α or oncogenic p110α mutants in a Boyden chamber Transwell assay. Cells expressing either helical domain or kinase domain mutations showed an increase in migration relative to cells expressing wild-type p110α in both the absence and the presence of EGF (Fig. 2*B*). Similarly, in a wound-healing assay, cells expressing wild-type p110α exhibited a similar rate of wound closure as control MDA-MB-231 cells. However, significantly faster wound closure was observed in cells expressing helical or kinase domain mutants of p110α cells, with >60% of the open area covered by the cells in a 20 h period (Fig. 2*C, top*). These differences were not due to differential proliferation, as rates of cell growth for cells expressing wild-type or mutant p110α were identical in both normal and reduced sera (data not shown). Quantification of wounding-induced migration during the first 4 h of wound healing showed that the migration rate was increased 1.5- to 2-fold in

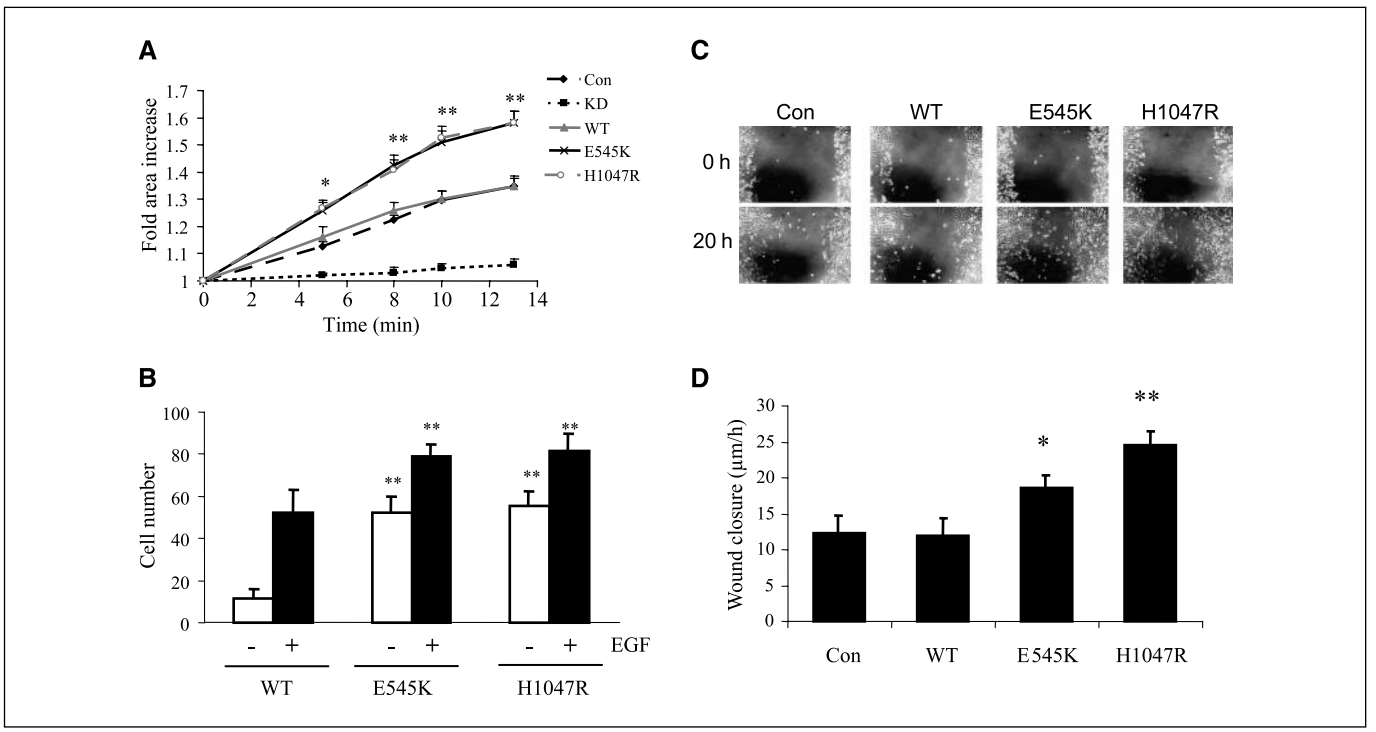

Figure 2. Expression of p110α mutants increases protrusion and migration. *A,* stable MDA-MB-231 cells expressing wild-type or mutant (helical domain: E545K; kinase domain: H1047R) bovine p110α were seeded in 35 mm dish coated with Matrigel. After 12 h to allow adhesion, the cells were starved for 4 h, and stimulated with 2.5 nmol/L EGF. Time-lapse images were collected every 20 s. The surface area of each cell was measured using ImageJ, and normalized to the initial cell area. Mean ± SE from 15 to 20 cells. *B,* cells were plated on collagen-coated Transwell chambers, and incubated for 4 h without or with EGF in the lower chamber. The cells were fixed and stained with 4′,6-diamidino-2-phenylindole, and the number of cells on the lower filter surface was counted. Mean ± SE from 3 experiments. *C,* monolayer cultures of stable MDA-MB-231 cells expressing wild-type or mutant bovine p110α were wounded with a P200 pipette tip. Phase-contrast images of the wound area were taken at time 0, 4, and 20 h. Images from the 0 h and the 20 h incubations are shown. *D,* the average rate of wound closure during the first 4 h of wound healing was calculated from three independent experiments. Mean ± SE and statistical significance were determined using a two-tailed students *t*-test. *, $P < 0.05$; **, $P < 0.01$ compared with cell expressing wild-type p110α.

Published OnlineFirst November 10, 2009; DOI: 10.1158/0008-5472.CAN-09-1968

cells expressing mutant p110α compared with cells expressing wild-type p110α (Fig. 2*C, bottom*). These data show that oncogenic mutations in p110α confer enhanced cell motility *in vitro*.

Helical domain mutation leads to increased directionality in MDA-MB-231 cells. To determine whether p110α helical and kinase domain mutations have an effect on chemotaxis, we used the Dunn chamber assay, which uses time-lapse video microscopy to monitor cell movement under the influence of a linear gradient of diffusing chemoattractant (17, 22). As expected, MDA-MB-231 cells moved in a nondirectional manner in the absence of EGF but showed clear directional movement in the presence of a 0 to 5 nmol/L EGF gradient (Fig. 3*A*). Interestingly, directional movement of cells expressing the kinase domain mutant was similar to that of cell expressing wild-type p110α (Fig. 3*B*). However, cells expressing the helical domain mutant exhibited significantly greater directionality than either the kinase domain mutant or wild-type cells ($P < 0.05$, Moore test; ref. 23; Fig. 3*B*). The comparison between cells expressing helical and kinase domain mutants was repeated at a lower dose of EGF (0-0.5 nmol/L) and yielded an even more obvious enhancement of chemotaxis in the helical domain cells ($P < 0.001$; Fig. 3*C*). Cells expressing the helical domain mutant also showed greater persistence (0.24 ± 0.03 versus 0.17 ± 0.02; $P < 0.05$), although the speed was not significantly different (data not shown). Taken together, these data show that whereas expression of either oncogenic mutant increases cell motility, expression of the helical domain mutant enhances directional sensing in a chemoattractant gradient. This prompted us to evaluate the potential differential effects of the two p110α mutations on intravasation and extravasation, two important components of metastasis *in vivo*.

Helical domain mutations causes enhanced intravasation compared with kinase domain mutations *in vivo*. Cells expressing wild-type or mutant p110α were injected into the mammary glands of SCID mice. Although no significant differences were observed in the proliferation rates of these cell lines *in vitro*, even under low serum conditions (data not shown), xenograft tumor-expressing helical or kinase domain mutants of p110α grew much faster than those expressing wild-type p110α (Fig. 4*A*). Tumors expressing the helical domain mutants showed a statistically significant enhancement in growth rate relative to tumors expressing the kinase domain mutants, although the difference was small when compared with the difference between mutant and wild-type p110α tumors. The rapid growth of tumors expressing kinase and

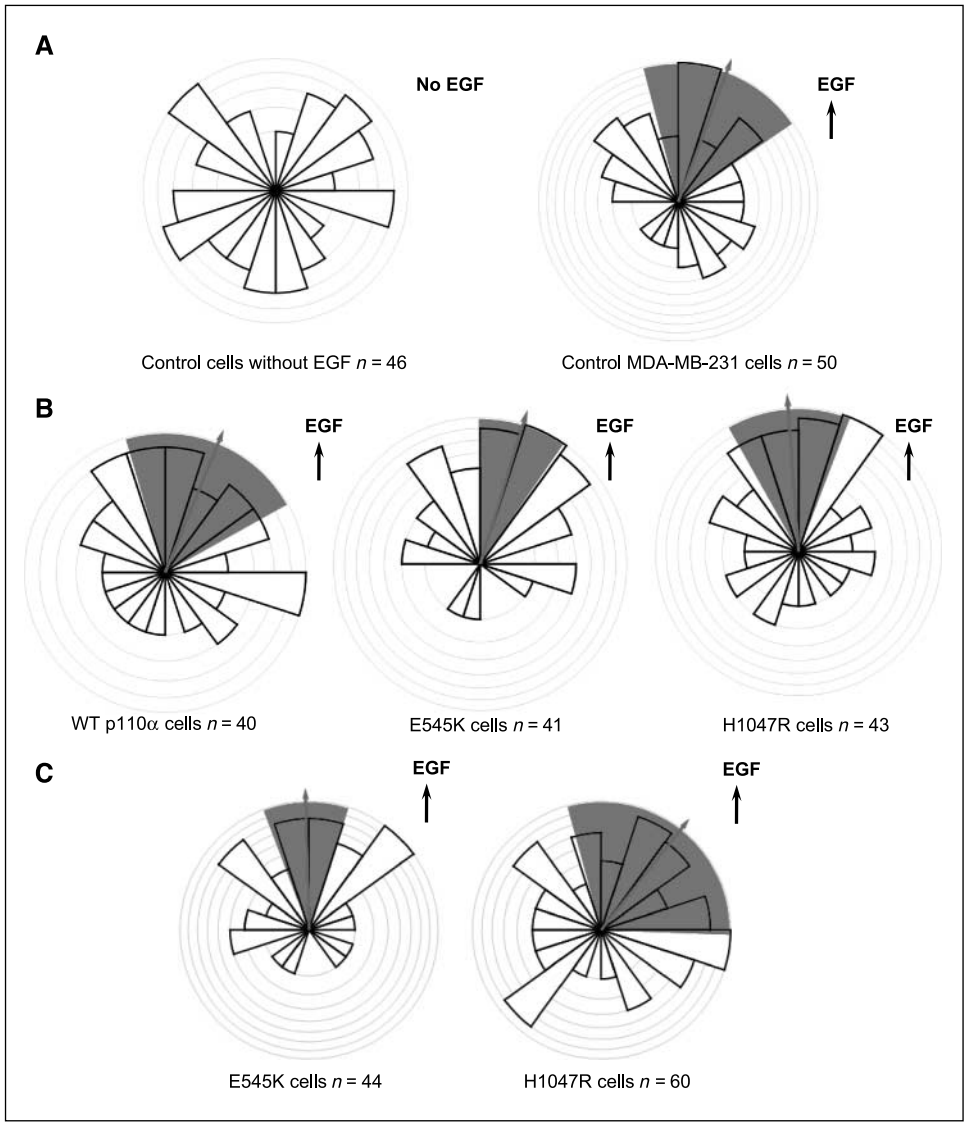

Figure 3. Expression of the helical domain mutant increases chemotaxis. Stable cell were placed in Dunn chambers in the presence or absence of EGF. Cell migration was recorded by time-lapse video microscopy, and analyses of migration and chemotaxis was done using Mathematica notebooks written and provided by Profs. G.A. Dunn and G.E. Jones (18). The bar height represents the proportion of cells moving in a particular direction, and the arrow and the shading indicate the mean direction of cell migration and its 95% confidence interval, respectively. *A,* chemotaxis of control MDA-MB-231 cells in the absence or presence of a 0 to 5 nmol/L EGF gradient. *B,* chemotaxis of cells expressing wild-type or mutant bovine p110α in a 0-5 nmol/L EGF gradient. 40-50 cells were counted for each group. $P < 0.005$ helical domain mutant (E545K) versus wild-type; $P < 0.05$ helical domain mutant (E545K) versus kinase domain mutant (H1047R) in the Moore test. *C,* chemotaxis of helical domain and kinase domain mutants in a 0 to 0.5 nmol/L EGF gradient. $P < 0.001$ in the Moore test.

Published OnlineFirst November 10, 2009; DOI: 10.1158/0008-5472.CAN-09-1968

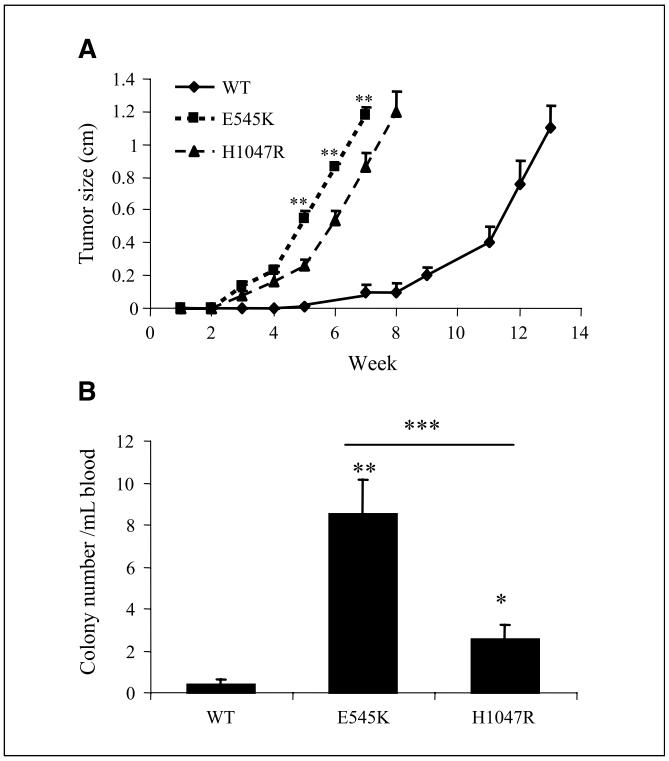

Figure 4. The helical domain mutation enhances tumor growth and *in vivo* intravasation. Cell lines expressing wild-type or mutant p110α were injected into the right mammary fat pads of SCID mice. *A,* spontaneous tumor size was recorded every week. **, $P < 0.01$ helical domain (E545K) versus kinase domain (H1047R). *B,* blood burden (intravasation) experiments were done once the tumor volumes reached 1.2-1.3 cm. Adherent tumor cells were counted 14 d after plating of the blood samples. Data are normalized for the blood volume for each sample. $n = 6$-11 mice per mutant type. **, $P < 0.01$ E545K versus wild-type; *, $P < 0.05$ H1047R versus wild-type; ***, $P < 0.01$ E545K versus H1047R in Mann-Whitney U test.

helical domain presumably involves interactions with stromal factors not seen in the *in vitro* proliferation experiments.

We assessed the ability of the tumor cells to intravasate into the blood by measuring the tumor cell blood burden as described (20). Tumor cell intravasation is affected by tumor size, and the blood tumor burdens were therefore measured when the xenograft tumors reached identical sizes (1.2-1.3 cm). Because of the differential growth rates, measurements were done after 7 weeks for tumors expressing helical domain mutants, 8 weeks for tumors expressing kinase domain mutants, and 13 weeks for tumors expressing wild-type p110α, such that tumor size was similar for each cell type. Colony counts from mice carrying helical domain or kinase domain mutants were higher than those with wild-type p110α (Fig. 4*B*). Interestingly, cells expressing the helical domain mutations exhibited a 3.4-fold higher rate of intravasation than cells expressing the kinase domain mutation regardless of the fact that mice carrying helical domain tumors were sacrificed 1 week earlier than mice carrying kinase domain tumors. These results strongly suggest that p110α oncogenic mutations increase breast cancer metastasis by promoting mobilization of mammary tumor cells into the circulation and that the helical domain mutation E545K promotes intravasation more robustly than the kinase domain mutation H1047R.

Helical domain mutations enhance tumor cell extravasation. The ability of tumor cells expressing wild-type or mutant p110α to extravasate into the lung was measured by injecting identical numbers of each cell line into the tail veins of SCID mice. The lungs were analyzed at 7 weeks, a time by which control MDA-MB-231 cells show measurable levels of lung metastasis (data not shown). As expected, metastatic foci were detectable in histologic sections from mice injected with cells expressing wild-type p110α (Fig. 5*A* and *B*). However, mice injected with cells expressing helical domain or kinase domain mutants of p110α E545K or H1047R cells developed extensive metastatic nodules evidenced by both gross and histologic analysis (Fig. 5*A* and *B*). The florid metastases caused high mortality in both groups (data not shown) and made it difficult to assess differences between two mutations. We therefore analyzed a separate cohort of mice at 4 weeks after tail vein injection. By this time, cells expressing the helical domain mutant showed a significantly higher level of metastasis than cells expressing the kinase domain mutant as evidenced by an increased number of metastatic foci and increased total metastatic area (Fig. 6). The dramatic differences in extravasation are unlikely to be explained by the slightly higher growth rate of helical domain versus kinase domain tumors and suggest that tumor cells expressing helical domain mutants of p110α show a much higher rate of migration from the vasculature into the lung.

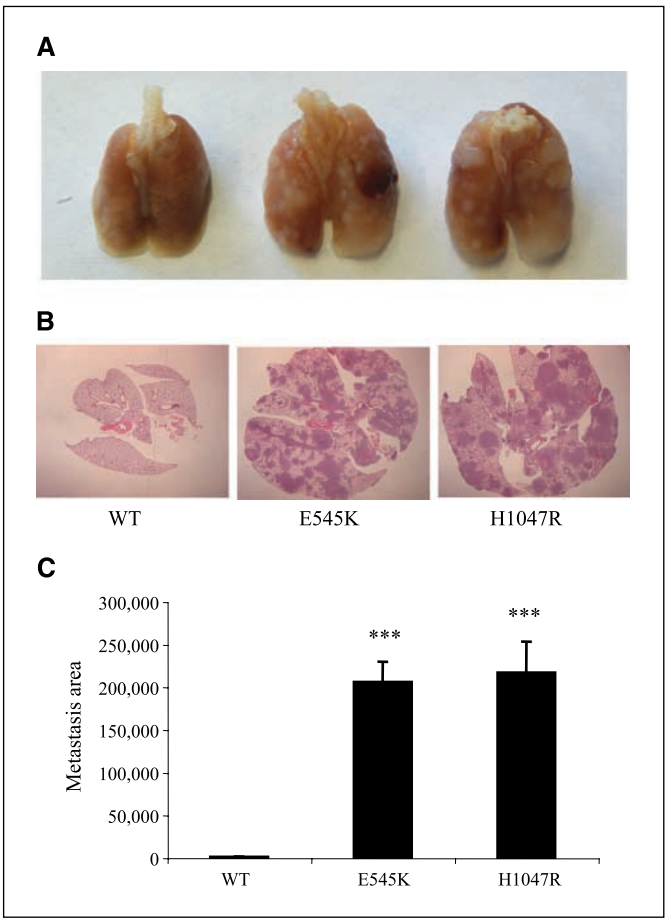

Figure 5. Tail vein injection of cells expressing mutant p110α leads to increased lung metastases. Stable cells expressing wild-type or mutant p110α (helical domain: E545K; kinase domain: H1047R) were injected into the lateral tail vein of SCID mice. Mice were sacrificed 7 wk after tail vein injection. *A,* lungs from control and mutant p110α mice. *B,* lung metastases were visualized by H&E staining. *C,* area of lung metastases were determined by ImageJ. ***, $P < 0.001$, relative to wild-type.

Published OnlineFirst November 10, 2009; DOI: 10.1158/0008-5472.CAN-09-1968

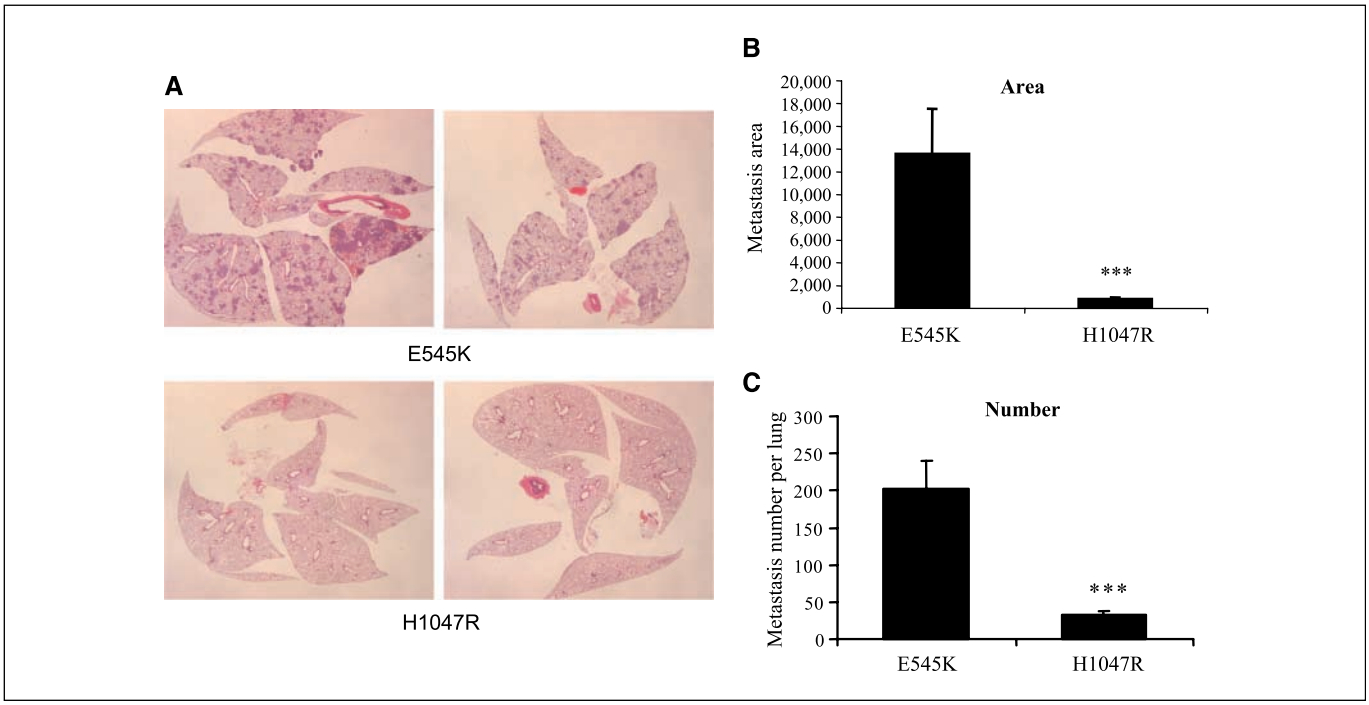

Figure 6. Increased lung metastasis in cells expressing helical domain versus kinase domain mutants of p110α. Stable cell lines were injected into the lateral tail vein of SCID mice as in Fig. 5. Mice were sacrificed 4 wk after tail vein injection. *A,* lung metastases were visualized by H&E staining. *B,* area of lung metastases was determined by ImageJ. *C,* the number of metastatic foci was determined by ImageJ. ***, $P < 0.001$, relative to E545K.

Discussion

The bulk of oncogenic mutations of p110α cluster in two hotspots: in an acid cluster in the helical domain (E542, E545, and Q546) and in the COOH terminus of the kinase domain (H1047). Both helical domain and kinase domain mutants of p110α cause increased lipid kinase activity in cells but by different mechanisms (2–5). The distinct mechanisms by which the helical domain and kinase domain mutants activate p85/p110 dimers might lead to distinct patterns of PIP_3 production in cells.

When we directly compared the effect of p110α helical domain versus kinase domain mutations in cell lines with otherwise identical genetic backgrounds, expression of the helical domain mutation led to increased chemotaxis *in vitro* and increased activity during *in vivo* metastasis assays. Cells expressing the helical domain mutant showed a small but significant increase in tumor growth rate compared with cells expressing the kinase domain mutant; both mutant cell lines produced tumors much faster than cells expressing wild-type p110α. However, the presence of tumor cells in the blood of animals with helical domain mutants was ~3-fold higher than in animals with kinase domain tumors. Similarly, metastasis to the lung was much faster after tail vein injection of helical domain opposed to kinase domain cells. These differences did not correspond to marked differences in Akt activation in the two cell lines, consistent with the idea that site-specific PI3K activity might be important in defining the phenotype of these mutants *in vivo*.

Several previous studies have compared signaling by overexpressed helical domain and kinase domain mutants of p110α. Overexpression of either NH_2-terminally tagged mutant in NIH 3T3 cells or mammary epithelial cells led to increased Akt activation, growth in soft agar, disruption of mammary acinar morphogenesis in three-dimensional culture, and tumor formation in a xenograft model (7–9). Similar results were seen in Ba/F3 mouse pro-B cells (10). In these studies, the phenotype produced by overexpression of either helical domain or kinase domain mutants were similar. A concern in some of these studies is the use of NH_2-terminal epitope tags, which stabilize p110α independently of binding to p85α and might obscure differences between the mutants (24). The COOH-terminal tag used in this study does not stabilize p110α, although it is possible that it could still have some unforeseen effect on signaling *in vivo*. Alternatively, Samuels and colleagues used a genetic strategy to silence the expression of helical domain or kinase domain mutants in human cell lines expressing a single copy of the mutant allele (DLD1 and HCT116 cells, respectively; ref. 12). The helical and kinase domain mutant lines both led to increased levels of tumor formation and metastasis in a xenograft model compared with the cells in which the mutant allele was ablated. However, a direct comparison of the *in vivo* phenotypes of the helical versus kinase domain mutants was difficult given that different cell lines were used. In a more recent study, knock-in of helical versus kinase domain mutations led to the activation of a similar range of downstream activators in MCF-10A cells (25). We also failed to see differences between helical domain and kinase domain mutants in responses such as protrusion or motility in the Boyden chamber, but we did see differences in complex behaviors such as *in vitro* chemotaxis in an EGF gradient and metastatic behavior *in vivo*.

In contrast, clear differences between helical domain and kinase domain mutants were seen in studies using retroviral expression of untagged p110α mutants in chicken fibroblasts; this method depends on endogenous p85 for stabilization of p110α and should not lead to overexpression. Although both mutations led to increased PI3K activity, expression of the kinase domain mutation

led to more robust Akt activation and foci formation in chicken fibroblasts and tumor production in the chicken embryo chorioallantoic membrane assay (11, 26). These studies are not consistent with our data, which show similar rates of tumor growth but increased metastatic behavior for the helical domain relative to the kinase domain mutants. However, multiple differences in the systems used (stromal factors, interactions with macrophages and other inflammatory cells, and cell type–specific and species-specific differences) could explain the different results.

Our data would suggest that, in human breast cancer cells identical in other respects, the presence of helical domain mutants of p110α would predict a more aggressive metastatic phenotype. The clinical evidence in support of this hypothesis is mixed. Several studies have suggested that mutations in p110α correlate with more severe disease in breast, colon, and endometrial cancers, but these studies did not separately compare helical domain versus kinase domain mutants (27–32). Helical domain mutants were found to predominate, relative to kinase domain mutations, in aggressive lobular breast carcinoma (33) and were found to be independently associated with poor prognosis in these tumors (34). Other studies found an association of kinase domain mutants, but not helical domains, with poor prognosis in breast and endometrial cancers (35–38). Finally, as mentioned earlier, kinase domain mutants were found at a higher rate than helical or C2 domain mutants (67% versus 19%) in tumors with a PTEN loss gene signature, which correlates with poor prognosis in several tumor types (13).

The relative effect of different p110α mutations on patient prognosis is likely to be complex and will undoubtedly also be influenced by the presence of other oncogenic mutations in a given tumor. For example, recent data from Vasudevan and colleagues suggest that, in some breast cancer lines expressing helical domain mutants of p110α, adaptations have occurred such that activation of Akt is minimal, and anchorage-independent growth relies on activation of PDK1 and SGK3 (39). In MDA-MB-231 cells, the Ras/ERK pathway is activated by mutations in both K-Ras and B-Raf.[2] K-Ras associates with distinct nonraft regions of the plasma membrane (6). Given that helical domain mutants of p110α show increased activity in the presence of oncogenic Ras, whereas kinase domain mutants do not (2), the presence of constitutively active K-Ras in MDA-MB-231 cells could lead to a localized activation of helical domain that would not occur in cells expressing kinase domain mutants of p85/p110α. It will be important to determine how such differential targeting regulates chemotaxis and metastatic behavior in breast cancer lines expressing mutant p110α.

Disclosure of Potential Conflicts of Interest

No potential conflicts of interest were disclosed.

Acknowledgments

Received 6/1/09; revised 8/21/09; accepted 9/23/09; published OnlineFirst 11/10/09.

Grant support: NIH grants GM55692 (J.M. Backer), CA113395 (J.S. Condeelis) and PO1 CA 100324 (J.M. Backer, A.R. Bresnick, J.E. Segall, and J.S. Condeelis), Albert Einstein Cancer Center grant P30 CA013330, and the Janey Fund (J.M. Backer). S. Goswami is the recipient of the Young Investigator Award from Breast Cancer Alliance.

The costs of publication of this article were defrayed in part by the payment of page charges. This article must therefore be hereby marked *advertisement* in accordance with 18 U.S.C. Section 1734 solely to indicate this fact.

We thank Dr. Gareth Jones (King's College London) for generous assistance with the Dunn chamber data analysis.

References

1. Engelman JA, Luo J, Cantley LC. The evolution of phosphatidylinositol 3-kinases as regulators of growth and metabolism. Nat Rev Genet 2006;7:606–19.
2. Zhao L, Vogt PK. Helical domain and kinase domain mutations in p110α of phosphatidylinositol 3-kinase induce gain of function by different mechanisms. Proc Natl Acad Sci U S A 2008;105:2652–7.
3. Miled N, Yan Y, Hon WC, et al. Mechanism of two classes of cancer mutations in the phosphoinositide 3-kinase catalytic subunit. Science 2007;317:239–42.
4. Chaussade C, Cho K, Mawson C, Rewcastle GW, Shepherd PR. Functional differences between two classes of oncogenic mutation in the PIK3CA gene. Biochem Biophys Res Commun 2009;381:577–81.
5. Carson JD, Van Aller G, Lehr R, et al. Effects of oncogenic p110α subunit mutations on the lipid kinase activity of phosphoinositide 3-kinase. Biochem J 2008; 409:519–24.
6. Eisenberg S, Henis YI. Interactions of Ras proteins with the plasma membrane and their roles in signaling. Cell Signal 2008;20:31–9.
7. Ikenoue T, Kanai F, Hikiba Y, et al. Functional analysis of PIK3CA gene mutations in human colorectal cancer. Cancer Res 2005;65:4562–7.
8. Zhao JJ, Liu Z, Wang L, Shin E, Loda MF, Roberts TM. The oncogenic properties of mutant p110α and p110β phosphatidylinositol 3-kinases in human mammary epithelial cells. Proc Natl Acad Sci U S A 2005;102:18443–8.
9. Isakoff SJ, Engelman JA, Irie HY, et al. Breast cancer-associated PIK3CA mutations are oncogenic in mammary epithelial cells. Cancer Res 2005;65:10992–1000.
10. Horn S, Bergholz U, Jucker M, et al. Mutations in the catalytic subunit of class IA PI3K confer leukemogenic potential to hematopoietic cells. Oncogene 2008;27: 4096–106.
11. Bader AG, Kang S, Vogt PK. Cancer-specific mutations in PIK3CA are oncogenic *in vivo*. Proc Natl Acad Sci U S A 2006;103:1475–9.
12. Samuels Y, Diaz LA, Jr., Schmidt-Kittler O, et al. Mutant PIK3CA promotes cell growth and invasion of human cancer cells. Cancer Cell 2005;7:561–73.
13. Saal LH, Johansson P, Holm K, et al. Poor prognosis in carcinoma is associated with a gene expression signature of aberrant PTEN tumor suppressor pathway activity. Proc Natl Acad Sci U S A 2007;104:7564–9.
14. Hill K, Welti S, Yu JH, et al. Specific requirement for the p85-110a phosphatidylinositol 3-kinase during epidermal growth factor-stimulated actin nucleation in breast cancer cells. J Biol Chem 2000;275:3741–4.
15. Dull T, Zufferey R, Kelly M, et al. A third-generation lentivirus vector with a conditional packaging system. J Virol 1998;72:8463–71.
16. Yip SC, Eddy RJ, Branch AM, et al. Quantification of PtdIns(3,4,5)P(3) dynamics in EGF-stimulated carcinoma cells: a comparison of PH-domain-mediated methods with immunological methods. Biochem J 2008;411:441–8.
17. Jones GE, Ridley AJ, Zicha D. Rho GTPases and cell migration: measurement of macrophage chemotaxis. Methods Enzymol 2000;325:449–62.
18. Ahmed T, Shea K, Masters JR, Jones GE, Wells CM. A PAK4-1 pathway drives prostate cancer cell migration downstream of HGF. Cell Signal 2008;20:1320–8.
19. Wyckoff J, Wang W, Lin EY, et al. A paracrine loop between tumor cells and macrophages is required for tumor cell migration in mammary tumors. Cancer Res 2004;64:7022–9.
20. Wyckoff JB, Jones JG, Condeelis JS, Segall JE. A critical step in metastasis: *in vivo* analysis of intravasation at the primary tumor. Cancer Res 2000;60:2504–11.
21. Yamaguchi H, Condeelis J. Regulation of the actin cytoskeleton in cancer cell migration and invasion. Biochim Biophys Acta 2007;1773:642–52.
22. Zicha D, Dunn G, Jones G. Analyzing chemotaxis using the Dunn direct-viewing chamber. Methods Mol Biol 1997;75:449–57.
23. Moore BR. A modification of the Rayleigh test for vector data. Biometrika 1980;67:175–80.
24. Yu J, Zhang Y, McIlroy J, Rordorf-Nikolic T, Orr GA, Backer JM. Regulation of the p85/p110 phosphatidylinositol 3′-kinase: stabilization and inhibition of the p110-α catalytic subunit by the p85 regulatory subunit. Mol Cell Biol 1998;18:1379–87.
25. Gustin JP, Karakas B, Weiss MB, et al. Knockin of mutant PIK3CA activates multiple oncogenic pathways. Proc Natl Acad Sci U S A 2009;106:2835–40.
26. Kang S, Bader AG, Vogt PK. Phosphatidylinositol 3-kinase mutations identified in human cancer are oncogenic. Proc Natl Acad Sci U S A 2005;102:802–7.
27. Berns K, Horlings HM, Hennessy BT, et al. A functional genetic approach identifies the PI3K pathway as a major determinant of trastuzumab resistance in breast cancer. Cancer Cell 2007;12:395–402.
28. Li SY, Rong M, Grieu F, Iacopetta B. PIK3CA mutations in breast cancer are associated with poor outcome. Breast Cancer Res Treat 2006;96:91–5.
29. Barault L, Veyrie N, Jooste V, et al. Mutations in the RAS-MAPK, PI(3)K (phosphatidylinositol-3-OH kinase)

Published OnlineFirst November 10, 2009; DOI: 10.1158/0008-5472.CAN-09-1968

signaling network correlate with poor survival in a population-based series of colon cancers. Int J Cancer 2008; 122:2255–9.

30. Kato S, Iida S, Higuchi T, et al. PIK3CA mutation is predictive of poor survival in patients with colorectal cancer. Int J Cancer 2007;121:1771–8.

31. Ogino S, Nosho K, Kirkner GJ, et al. PIK3CA mutation is associated with poor prognosis among patients with curatively resected colon cancer. J Clin Oncol 2009;27: 1477–84.

32. Salvesen HB, Carter SL, Mannelqvist M, et al. Integrated genomic profiling of endometrial carcinoma associates aggressive tumors with indicators of PI3 kinase activation. Proc Natl Acad Sci U S A 2009;106:4834–9.

33. Buttitta F, Felicioni L, Barassi F, et al. PIK3CA mutation and histological type in breast carcinoma: high frequency of mutations in lobular carcinoma. J Pathol 2006;208:350–5.

34. Barbareschi M, Buttitta F, Felicioni L, et al. Different prognostic roles of mutations in the helical and kinase domains of the PIK3CA gene in breast carcinomas. Clin Cancer Res 2007;13:6064–9.

35. Lai YL, Mau BL, Cheng WH, Chen HM, Chiu HH, Tzen CY. PIK3CA exon 20 mutation is independently associated with a poor prognosis in breast cancer patients. Ann Surg Oncol 2008;15:1064–9.

36. Gonzalez-Angulo AM, Stemke-Hale K, Palla SL, et al. Androgen receptor levels and association with PIK3CA mutations and prognosis in breast cancer. Clin Cancer Res 2009;15:2472–8.

37. Catasus L, Gallardo A, Cuatrecasas M, Prat J. PIK3-CA mutations in the kinase domain (exon 20) of uterine endometrial adenocarcinomas are associated with adverse prognostic parameters. Mod Pathol 2008;21: 131–9.

38. Catasus L, Gallardo A, Cuatrecasas M, Prat J. Concomitant PI3K-AKT and p53 alterations in endometrial carcinomas are associated with poor prognosis. Mod Pathol 2009;22:522–9.

39. Vasudevan K, Barbie D, Davies M, et al. AKT-independent signaling downstream of oncogenic PIK3CA mutations in human cancer. Cancer Cell 2009;16:21–32.

Cancer Research
The Journal of Cancer Research (1916–1930) | The American Journal of Cancer (1931–1940)

AACR American Association for Cancer Research

Differential Enhancement of Breast Cancer Cell Motility and Metastasis by Helical and Kinase Domain Mutations of Class IA Phosphoinositide 3-Kinase

Huan Pang, Rory Flinn, Antonia Patsialou, et al.

Cancer Res 2009;69:8868-8876. Published OnlineFirst November 10, 2009.